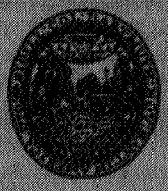

DARTMOUTH COLLEGE
Thayer School of Engineering
Hanover, New Hampshire

On the Equilibrium of the Magnetopause Current Layer

Shin-Yi Su and Bengt U.Ö. Sonnerup

Radiophysics Laboratory
Dartmouth College
Hanover, New Hampshire 03755

June 1970

This work was supported by the National Aeronautics and Space Administration under Grant NGR-30-001-011.

On the Equilibrium of the Magnetopause Current Layer

Shin-Yi Su and Bengt U.Ö. Sonnerup

Radiophysics Laboratory
Dartmouth College
Hanover, New Hampshire 03755

June 1970

This work was supported by the National Aeronautics and Space Administration under Grant NGR-30-001-011.

Abstract

Confinement of a uniform magnetic field by a warm hydrogen plasma with an average velocity parallel to the confined field is studied. It is found that for a given proton temperature equilibria exist whenever the electron temperature exceeds a certain critical value. Thus, at the magnetopause equilibrium states may exist near the nose of the magnetosphere but usually not along the tail. A comparison is made with the results of Parker and Lerche. The fallacy of Lerche's non-existence proof is pointed out. The properties of the equilibrium solutions are discussed. Finally, the equilibrium confinement with the incident streaming plasma tangential to the magnetopause but perpendicular to the confined field is treated. It is concluded that in the geomagnetic equatorial plane magnetopause equilibria may occur on the afternoon side but not on the morning side of the magnetosphere.

Introduction

In two recent papers, Parker [1967 a,b] sets out the reasons why the magnetopause may not be in a state of equilibrium along the geomagnetic tail. He considers the case where the magnetic field outside the magnetopause is sufficiently weak to be neglected. Thus the problem is that of the confinement of a uniform magnetic field by an incident nonmagnetic plasma beam. Parker's conclusions may be summarized as follows: The electric field contained in other magnetopause models [Ferraro, 1952; Dungey, 1958; Rosenbluth and Garwin, 1963; Davis, 1968, 1969] in order to cause electrons and protons to turn around at the same depth inside the layer, is nullified by cold plasma supplied from the ionosphere. With the electric field equal to zero, electrons and protons turn at different depths. When the incident plasma has an average velocity along the confined uniform field B_x, this leads to a proton current along that field as shown in Fig. 1. The pressure of the resulting induced transverse magnetic field B_y must be balanced by the electron pressure in the incident beam in order for an equilibrium to exist. Parker gives an estimate of the necessary minimum electron pressure and concludes that a sufficient pressure may not always be available in the solar wind plasma especially along the geomagnetic tail.

Later Lerche [1967, 1968] generalized Parker's analysis by including the effects of thermal motions in the incident plasma in a rigorous manner. He concluded that no static equilibrium is possible for reasonable values of the electron pressure. The error in Lerche's analysis is pointed out in the

appendix. In this paper we show that equilibrium solutions do exist provided that the electron pressure is sufficiently large. The requisite minimum pressure is in qualitative agreement with Parker's prediction. The properties of the resulting magnetopause equilibria are calculated and discussed.

The main part of the present paper deals with the case of plasma flow along the confined magnetic field. However, a brief discussion is also given of the situation where the streaming plasma is tangential to the magnetopause but perpendicular to the confined field, as is the case in the geomagnetic equatorial plane. It is shown that magnetopause equilibria of Parker's type may exist on the afternoon side but not on the morning side of the magnetosphere.

Analysis

In the following analysis, the magnetic field configuration and notation used in Lerche's analysis will be adopted with the exception that a right-hand rather than a left-hand coordinate system is used. The confined magnetic field, B_x, is directed in the x-direction and the induced transverse magnetic field, B_y, in the y-direction. All equilibrium quantities depend only on the z-coordinate which is measured along the direction normal to the interface. The field configuration is shown in Fig. 1. The plasma to be considered has a distribution function at $z = -\infty$ where $\underset{\sim}{B} = 0$, given by

$$f_{p,e} = n_o\left(\frac{1}{2\pi m_{p,e} kT_{p,e}}\right)^{\frac{1}{2}} e^{-\frac{m_{p,e} v_z^2}{2kT_{p,e}}} \delta(v_x - U)\delta(v_y), \qquad (1)$$

so that n_o is the particle density at $z = -\infty$. Also k is the Boltzmann constant and m and T are the mass and the temperature, respectively. The subscripts p and e denote the proton and electron species of the plasma, respectively. The δ-functions are Dirac delta functions. It is seen that U is the average velocity in the x-direction, i.e., along the confined magnetic field. Equation (1) shows that, apart from the streaming velocity, the incident plasma is assumed to be cold in the x- and y-directions, but warm in the z-direction. The former assumption is made for mathematical convenience, the latter in order to incorporate a component of the particle pressure perpendicular to the layer. The pressure associated with thermal

motions parallel to the layer is not expected to change the conclusions of the analysis in a substantial way. The distribution function given in Eq. (1) is a member of the family of distribution functions considered by Lerche in his analysis.

The existence of a non-energetic background plasma will assure charge neutrality so that Poisson's equation is automatically satisfied. Thus, the only Maxwell equation of importance in this case is Ampère's law, i.e., in CGS units,

$$\nabla \times \underset{\sim}{B} = \frac{4\pi e}{c} \sum_{p,e} \int \underset{\sim}{v} f_{p,e} \, d\underset{\sim}{v}. \tag{2}$$

Here $\sum_{p,e}$ denotes a summation of the proton and the electron species. Also, e is the magnitude of the electron charge and c is the speed of light. Parker and Lerche assume that no energetic trapped particles are present. Thus, contributions from such particles to the current density on the right-hand side of Eq. (2) were excluded. The validity of this assumption in the magnetospheric application is questionable. However, to facilitate comparison with Parker's and Lerche's work, we will use the same assumption in this paper. Thus, we transform the integration on the right-hand side of Eq. (2) from a local point within the current layer to the point at $z = -\infty$ before substituting Eq. (1) into Eq. (2). This will assure that only particles which originated at $z = -\infty$ are included in the calculation of the current density.

After straightforward but lengthy calculations, the two nontrivial components of Eq. (2) may be written in the follow-

ing dimensionless form:

$$\frac{d^2G^*}{dz^{*2}} = - \frac{\partial V^*}{\partial G^*} , \tag{3}$$

$$\frac{d^2F^*}{dz^{*2}} = - \frac{\partial V^*}{\partial F^*} , \tag{4}$$

where

$$V^* = \frac{1}{2}T_p^* \, e^{\gamma}\{1 - \varepsilon \, \mathrm{erf}(\sqrt{\gamma})\} + \varepsilon T_p^* \sqrt{\gamma/\pi} + \frac{1}{2}T_e^* e^{\beta}. \tag{5}$$

Here the following notation is used:

$$\frac{dG}{dz} = - B_y, \qquad \frac{dF}{dz} = - B_x,$$

$$G^* = \frac{eG}{m_p cU}, \qquad F^* = \frac{eF}{m_p cU},$$

$$T_p^* = \frac{kT_p}{\frac{1}{2}m_p U^2}, \qquad T_e^* = \frac{kT_e}{\frac{1}{2}m_p U^2},$$

$$z^* = z/\left(\frac{m_p c^2}{4\pi n_o e^2}\right)^{\frac{1}{2}}, \qquad \mu = \frac{m_p}{m_e},$$

$$\gamma = [1 - (G^* + 1)^2 - F^{*2}]/T_p^*,$$

$$\beta = \left[\frac{1}{\mu^2} - \left(G^* - \frac{1}{\mu}\right)^2 - F^{*2}\right]\mu/T_e^*.$$

The parameter ε in Eq. (5) is equal to 1 when $\gamma > 0$ and equal to zero when $\gamma < 0$. F^* and, apart from a sign, G^* are the components of the dimensionless vector potential corresponding to

the confined and the transverse magnetic field, respectively. The derivation of Eqs. (3), (4) and (5) involves the substitution of Eq. (1) into Lerche's Eq. (13) [Lerche, 1967]. See also Su [1969]. In obtaining Eqs. (3) to (5), we have assumed that $G < 0$. In the case analyzed here, it can be shown that $G > 0$ corresponds to $m_p T_p^* < m_e T_e^*$, a situation of little practical interest.

Eqs. (3) and (4) can be integrated once to yield

$$\left(\frac{dG^*}{dz^*}\right)^2 + \left(\frac{dF^*}{dz^*}\right)^2 = B_o^{*2} - 2V^*, \tag{6}$$

where B_o^* is the normalized uniform magnetic-field magnitude at $z \to +\infty$, or equivalently at $F^* = +\infty$ where $V^* = 0$.

An analogy used by Parker in his analysis [1967a] helps in understanding Eqs. (3), (4), (5), and (6): Consider the motion of a fictitious particle in the G^*F^* plane with z^* playing the role of time. Equations (3) and (4) state that the only force influencing the motion of the particles is derived from the "potential" V^* given by Eq. (5). The conservation of the particle's "energy" is expressed by Eq. (6).

The problem is "time" reversible and the equilibrium confinement corresponds to a particle trajectory which satisfies the following initial and final conditions:

Initial conditions; position: $F^* = +\infty$, $G^* = -$ const.
velocity: $\frac{dF^*}{dz^*} = +B_o^*$, $\frac{dG^*}{dz^*} = 0$.

Final conditions; position: $F^* \to 0$, $G^* = 0$.
velocity: $\frac{dF^*}{dz^*} = 0$, $\frac{dG^*}{dz^*} = 0$.

With these conditions the problem can be viewed as follows: A

particle initially located at a large "distance" F^* from the origin moves with "velocity" B_o^* along a line $G^* = -$ constant toward the origin. Near the origin it encounters two potential hills. One of them is the proton hill centered at $F^* = 0$, $G^* = -1$. The other is the electron hill centered at $F^* = 0$, $G^* = +1/1840$. The desirable path is such that the final destination of the particle is the origin which is located between the two hills. Furthermore, the initial "velocity" B_o^* is chosen in such a manner that the particle will reach the origin with zero velocity. A side view of the shape of the potential hills at $F^* = 0$ for $T_p^* = T_e^* = 0.5$ is shown in Fig. 2a.

For a given pair of proton and electron temperatures, say $T_p^* = T_e^* = 0.5$, the shape of the two potential hills is determined via Eq. (5), and so is the initial "velocity" B_o^* via Eq.(6). It is then required to find the initial G^* value that will produce the desired trajectory. Clearly this initial G^* value plays the role of the "impact parameter". If the initial $|G^*|$ is chosen too large, the particle has a large "angular momentum". It will miss the origin on the low side. On the other hand, a too small initial $|G^*|$ value will give a too small angular momentum and the particle will miss the origin on the opposite side. Between these two trajectories there is one which reaches the origin. The initial G^* value of this trajectory is found by trial and error. A diagram showing the three trajectories discussed above is shown in Fig. 2b.

The previous paragraph illustrates the case where an equilibrium solution does exist. However, if for a given electron

temperature the proton temperature is made sufficiently large then the influence of the proton potential hill becomes sufficiently strong so that all trajectories with an initial G* value in the range $-1 < G^* < 0$ will miss the origin on the upper side or will turn back without reaching the origin. Since trajectories with an initial G* value of less than - 1 always pass on the lower side of the proton hill and thus do not come close to the origin this means that no equilibrium solution exists.

The numerical solution of the desired trajectory in the F*G* plane is obtained by applying the Runge-Kutta method of integration to the following equation

$$\frac{d^2F^*}{dG^{*2}} = \left[1 + \left(\frac{dF^*}{dG^*}\right)^2\right] \frac{\frac{\partial V^*}{\partial G^*}\frac{dF^*}{dG^*} - \frac{\partial V^*}{\partial F^*}}{B_o^{*2} - 2V^*} . \tag{7}$$

Equation (7) is obtained by combining Eqs. (3) and (4). It should be noted that the right-hand member of Eq. (7) is of the form 0/0 at the origin. To avoid computer difficulties in dealing with the region near the origin, an approximate analytic solution, valid in that region, is used. This solution is then matched to the numerical solution. It is easy to show that the approximate analytic solution is given by

$$\frac{dF^*}{dz^*} = \pm [1 + \mu]^{\frac{1}{2}} F^* ,$$

$$\frac{dG^*}{dz^*} = \pm [B_o^{*2} - 2V^* - (1 + \mu)F^{*2}]^{\frac{1}{2}} .$$

Discussion

Since the proton and electron temperatures determine the shape of the potential hills shown in Fig. 2b, the numerical solution of Eq. (7) closely depends on the proton and electron temperatures. The region above curve 1 in Fig. 3 indicates the range of these temperatures for which equilibrium solutions exist. Parker [1967a] has estimated the minimum electron pressure needed for equilibrium. His result, shown by curve 2 in Fig. 3, is seen to be in qualitative agreement with the present work.

When the results of the previous analysis are applied to the magnetopause, it is found that equilibrium states may or may not exist near the nose of the magnetosphere but that they usually do not exist along the tail. In the former location, typical normalized proton and electron temperatures are [Olbert et al., 1967; Olbert, 1968], $T_p^* \simeq 0.5 - 2.5$ and $T_e^* \simeq 0.25 - 1$, e.g., corresponding to $T_p \simeq 3 \times 10^5 - 2 \times 10^6$ °K, $T_e \simeq 2 \times 10^5 - 6 \times 10^5$ °K, and $U \simeq 100$ Km/sec. In the latter location, $T_p^* \simeq 0.002 - 0.06$ and $T_e^* \simeq 0.04 - 0.06$, e.g., corresponding to $T_p \simeq 10^4 - 3 \times 10^5$ °K, $T_e \simeq 2 \times 10^5$ °K $- 3 \times 10^5$ °K, and $U \simeq 300$ Km/sec. The temperature ranges are shown by the rectangles in Fig. 3.

If magnetopause currents of the type discussed by Parker [1967a] are important, then the associated magnetic-field component transverse to the earth's field would have opposite directions above and below the equatorial plane, as shown in

Fig. 1. This provides a simple experimental test of the validity of Parker's model. Observations of the sense of the transverse magnetic field at the magnetopause have been reported by Sonnerup and Cahill [1968]. For boundaries identified by them as tangential discontinuities the direction of the transverse field appears random. For boundaries identified as rotational discontinuities, a relationship appears to exist between the sense of the transverse field and the location above and below the equatorial plane. However, this relationship is opposite to the one predicted by Parker's model. It should be pointed out that most of the cases reported by Sonnerup and Cahill involved a substantial magnetic field outside the magnetopause, a situation in which the applicability of Parker's model is questionable.

In comparing predictions from Parker's magnetopause model with observations it should also be remembered that the model has no currents associated with trapped particles. Alpers [1969] has discussed a situation where trapped energetic particles contribute currents along the confined magnetic field in such a manner that the transverse field, B_y, is completely suppressed. In such a case no difficulties arise in finding equilibrium solutions. It is conceivable that a number of mechanisms for the trapping of solar-wind particles are operative at the magnetopause. Furthermore, Ferraro and Davis [1968] and Davis [1968, 1969] have shown that the existence of even a small electric field normal to the magnetopause can be of substantial importance in helping to bring about an equilibrium.

Polar plots of the magnetic field vector inside the equilibrium magnetopause have been obtained from the calculations presented here and are shown in Fig. 4. It is interesting to note that for certain proton and electron temperatures, the total field magnitude does not decrease monotonically across the magnetopause.

Finally, it is observed that the analysis presented here can be used in principle to discuss the equilibrium confinement of a vacuum magnetic field by a streaming non-magnetized plasma with an average velocity parallel to the interface but forming an angle with the confined field. For such a case, the equilibrium confinement corresponds to a particle trajectory in Fig. 2b such that the initial velocity vector forms a non-zero angle with the F* axis. A complete analysis is not yet available. However, we may discuss the case where the trajectory in Fig. 2b lies along the line F* = 0. This corresponds to the situation where the incident stream is perpendicular to the confined field. For trajectories along the negative G* axis solutions exist when the electron temperature exceeds the value given by curve 3 in Fig. 3. For trajectories along the positive G* axis no equilibria are possible in the temperature range covered by Fig. 3. These results imply that in the equatorial plane equilibria may occur on the afternoon side but not on the morning side of the magnetosphere. The different behavior on the afternoon and the morning side is related to the fact that the proton orbits inside the magnetopause are

direct, i.e., nonlooped, in the former case and retrograde, i.e., looped, in the latter. The net current associated with retrograde orbits is much smaller than that associated with direct ones. If real, this asymmetry of the magnetopause may have important geophysical consequences [see e.g., Piddington, 1969].

Acknowledgement

The research was supported by NASA under grant NGR-30-001-011 to Dartmouth College.

Appendix

The purpose of this appendix is to demonstrate that there is a sign error in Eq. (52) of Lerche [1967].

The distribution functions Φ_p and Φ_e in Eq. (41) of Lerche's paper [1967] are even functions of the arguments w_o and v_o, where w_o is the velocity component normal to the interface and v_o the component parallel to it but perpendicular to the confined field. Thus, it is reasonable to assume Φ_p and Φ_e to be of the form

$$\Phi_p(w_o,v_o) = f_p(w_o^2,v_o^2),$$

$$\Phi_e(w_o,v_o) = f_e(w_o^2,v_o^2).$$

Then Lerche's Eq. (41) becomes

$$R(F) = \int_o^\infty dy \int_{\theta=o}^{\theta=\infty} \{d(ch\theta(2\alpha Fy)^{\frac{1}{2}}) f_p[sh^2\theta(2\alpha Fy), (y + \frac{\alpha F}{2})^2] + d(sh\theta(2\alpha Fy)^{\frac{1}{2}} f_p[ch^2\theta(2\alpha Fy), (y - \frac{\alpha F}{2})^2]\} - \int_o^\infty dy \int_{\theta=o}^{\theta=\infty} \{d(ch\theta(2\alpha\mu Fy)^{\frac{1}{2}}) f_e[sh^2\theta(2\alpha\mu Fy), (y + \frac{\alpha\mu F}{2})^2] + d(sh\theta(2\alpha\mu Fy)^{\frac{1}{2}}) f_e[ch^2(2\alpha\mu Fy), (y - \frac{\alpha\mu F}{2})^2]\}. \quad (A\text{-}1)$$

The notation is defined in Lerche's paper. Now let

$$\left.\begin{aligned} \zeta &= ch\theta(2\alpha Fy)^{\frac{1}{2}} \\ \eta &= sh\theta(2\alpha Fy)^{\frac{1}{2}} \end{aligned}\right\} \text{ in the proton part,}$$

and

$$\left.\begin{aligned} \zeta &= ch\theta(2\alpha\mu Fy)^{\frac{1}{2}} \\ \eta &= sh\theta(2\alpha\mu Fy)^{\frac{1}{2}} \end{aligned}\right\} \text{ in the electron part.}$$

Eq. (A-1) then reads

$$\begin{aligned} R(F) = \int_0^\infty dy \Big\{ & \int_{(2\alpha Fy)^{\frac{1}{2}}}^\infty d\zeta f_p[\zeta^2 - 2\alpha Fy, (y + \tfrac{\alpha F}{2})^2] \\ & + \int_0^\infty d\eta f_p[\eta^2 - 2\alpha Fy, (y - \tfrac{\alpha F}{2})^2]\Big\} \\ & - \int_0^\infty dy\Big\{ \int_{(2\alpha\mu Fy)^{\frac{1}{2}}}^\infty d\zeta f_e[\zeta^2 - 2\alpha\mu Fy, (y + \tfrac{\alpha\mu F}{2})^2] \\ & + \int_0^\infty d\eta f_e[\eta^2 - 2\alpha\mu\, Fy, (y - \tfrac{\alpha\mu F}{2})^2]\Big\}. \end{aligned}$$

Therefore,

$$\begin{aligned} \left(\frac{dR}{d(F)^{\frac{1}{2}}}\right)_{F=o} &= -(2\alpha)^{\frac{1}{2}} \int_o^\infty y^{\frac{1}{2}} dy\, f_p(0, y^2) \\ &\quad + (2\alpha\mu)^{\frac{1}{2}} \int_o^\infty y^{\frac{1}{2}}\, dy\, f_e(0, y^2). \end{aligned} \qquad \text{(A-2)}$$

The form of the right-hand side of Eq. (A-2) is the same as that of Lerche's Eq. (52) but the sign is opposite. With the sign given by Eq. (A-2) Lerche's non-existence proof becomes invalid.

References

Alpers, W., Steady state charge neutral models of the magnetopause, Astrophys. and Space Sci., 5, 425, 1969.

Davis, C.M., The boundary layer between a cold plasma and a confined magnetic field when the plasma is not normally incident on the boundary, Planetary Space Sci., 16, 1249, 1968.

Davis, C.M., The structure of the magnetopause, Planetary Space Sci., 17, 333, 1969.

Dungey, J.W., Cosmic Electrodynamics, Cambridge U.P., Cambridge, 1958.

Ferraro, V.C.A., On the theory of the first phase of a geomagnetic storm: a new illustrative calculation based on an idealized (plane not cylindrical) model field distribution, J. Geophys. Res., 57, 15, 1952.

Ferraro, V.C.A., and C.M. Davis, Discussion of paper by E.N. Parker, 'Confinement of a magnetic field by a beam of ions', J. Geophys. Res., 73, 3605, 1968.

Lerche, I., On the boundary layer between a warm, streaming plasma and a confined magnetic field, J. Geophys. Res., 72, 5295, 1967.

Lerche, I., Reply to Hurley's comment, J. Geophys. Res., 73, 3602, 1968.

Olbert, S., A. Egidi, G. Moreno, L.G. Pai, Summary of final results from the MIT plasma experiment on IMP-1, Trans. Am. Geophys. Union, 48, 177, 1967.

Olbert, S., Summary of experimental results from MIT detector on IMP-1, Physics of the Magnetosphere, edited by R.L. Carovillano, J.F. McClay, and H.R. Radoski, D. Reidel Pub. Co., Dordrecht - Holland, 1968.

Parker, E.N., Confinement of a magnetic field by a beam of ions, J. Geophys. Res., 72, 2315, 1967a.

Parker, E.N., Small-scale nonequilibrium of the magnetopause and its consequences, J. Geophys. Res., 72, 4365, 1967b.

Piddington, J.H., Cosmic Electrodynamics, Wiley-Interscience Pub., New York, (1969), p 139.

Rosenbluth, M.N., R. Garwin, and A. Rosenbluth, Infinite conductivity theory of the pinch, Plasma Physics and Thermonuclear Research in Progress in Nuclear Energy, Ser. XI, 2, edited by Longmire, Tuck, and Thompson, Macmillian Co, New York, 1963.

Sonnerup, B.U.Ö., and L.J. Cahill, Jr., Explorer 12 observations of the magnetopause current layer, J. Geophys. Res., 73, 1757, 1968.

Su, S.Y., Ph.D. Thesis, Dartmouth College, 1969.

Figure Captions

Fig. 1. Schematic representation of the boundary between the streaming solar-wind plasma and the geomagnetic field. The currents i_p and i_e result from the different penetration depths into the magnetic field of the streaming protons and electrons. These currents induce a magnetic field along the y direction. This transverse field, B_t, has opposite directions above and below the equatorial plane.

Fig. 2. (a) A cross section of the potential distribution, given by Eq. (5), as a function of G* for F* = 0.
(b) Potential hills and integration pathes in the F*G* plane. Curve 1: Too large initial |G*| value. Curve 2: Correct initial |G*| value. Curve 3: Too small initial |G*| value.

Fig. 3. Normalized proton and electron temperatures ($T_p^* \equiv 2kT_p/m_pU^2$; $T_e^* \equiv 2kT_e/m_pU^2$) required for equilibrium. The curves represent the boundary between equilibrium and non-equilibrium regions obtained from the present calculation (curve 1), from Parker's formula $T_e^* = T_p^*[(1+1/T_p^*)^{\frac{1}{2}} - 1]$ (curve 2), and for the case of flow transverse to the confined field (curve 3).

Fig. 4. Polar plots of the magnetic field vector inside the equilibrium magnetopause.

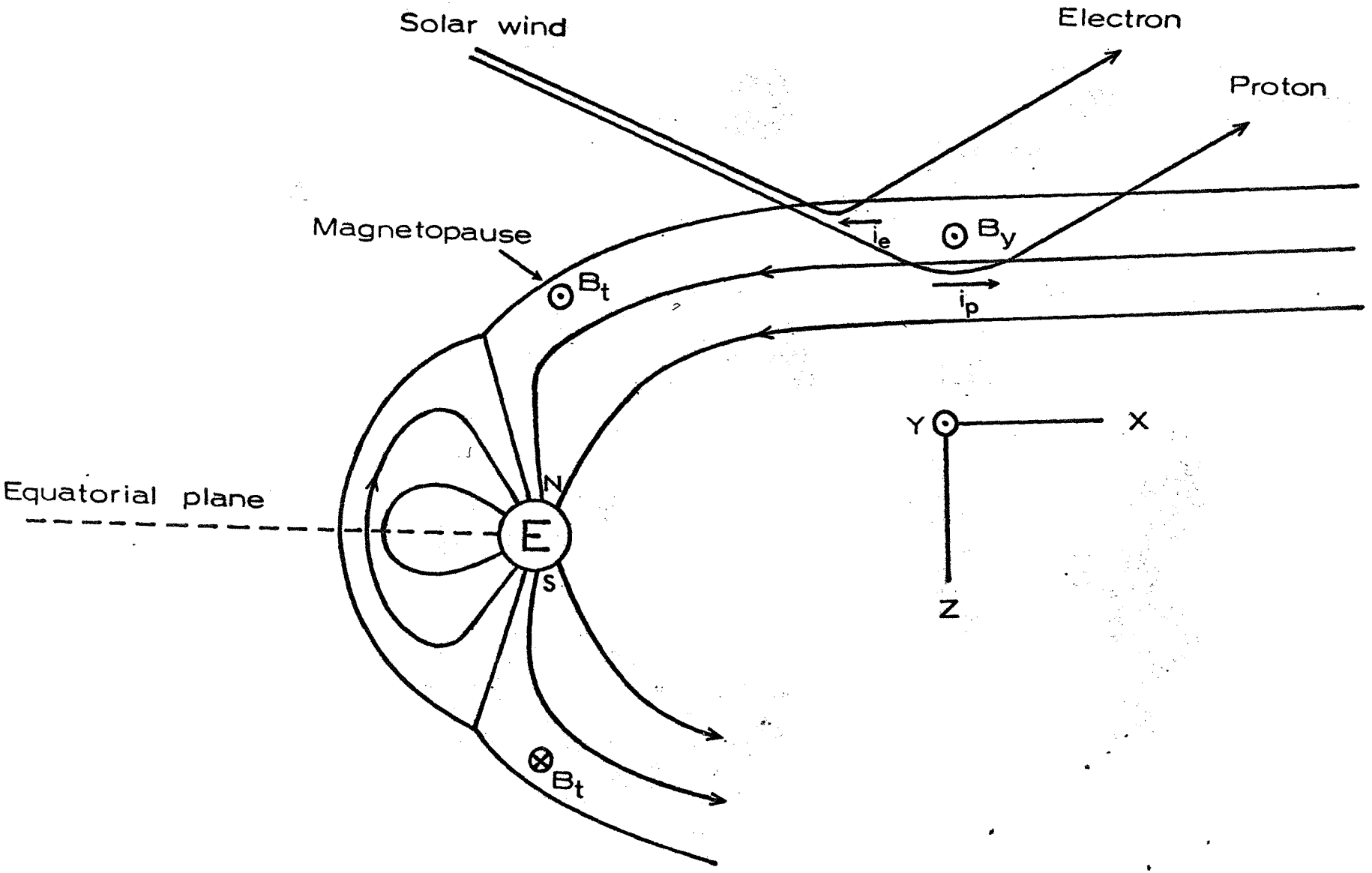
Solar wind
Electron
Proton
Magnetopause
i_e
B_y
B_t
i_p
Y
X
Z
Equatorial plane
N
E
S
B_t

FIGURE 1

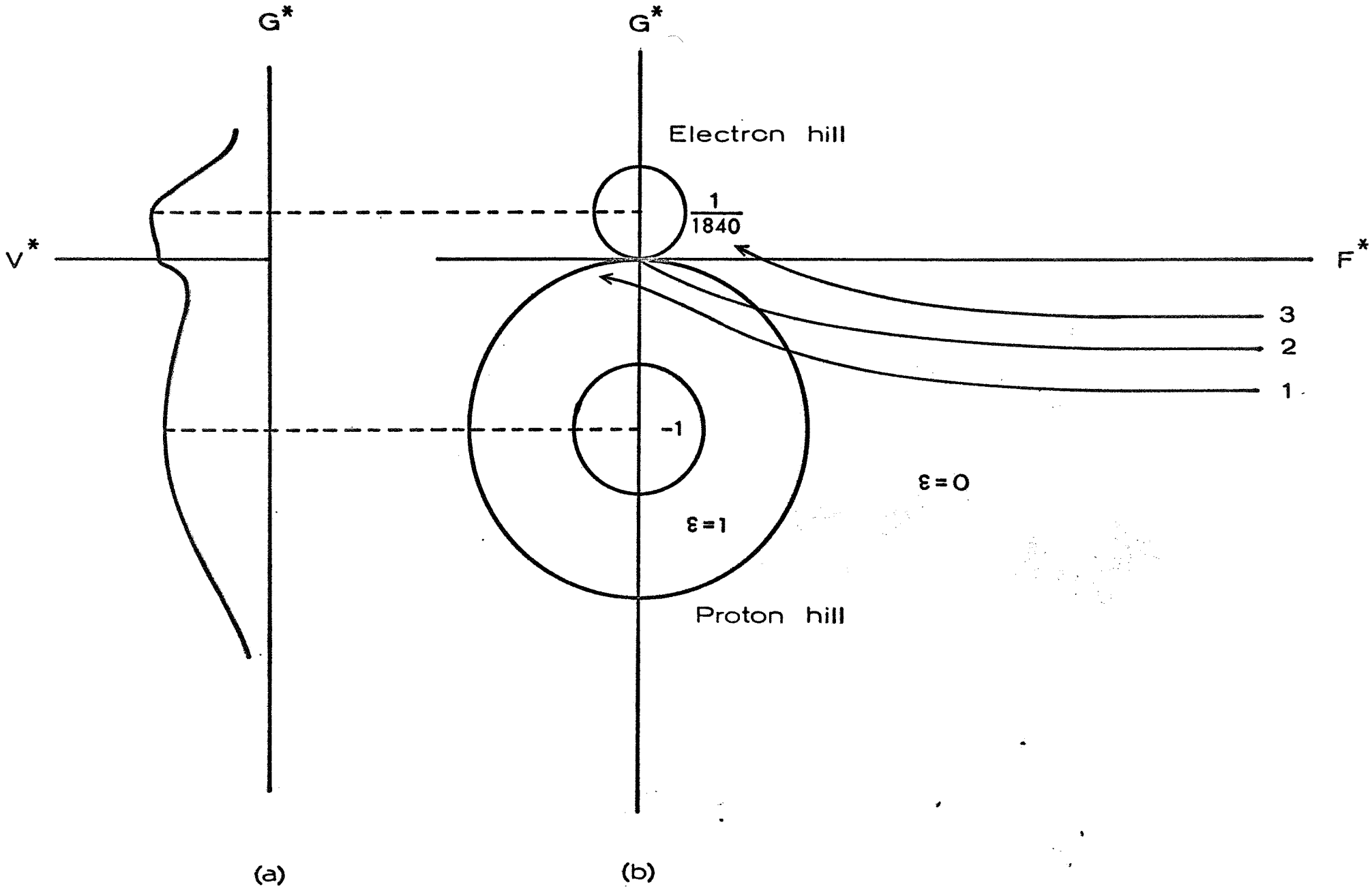

FIGURE 2

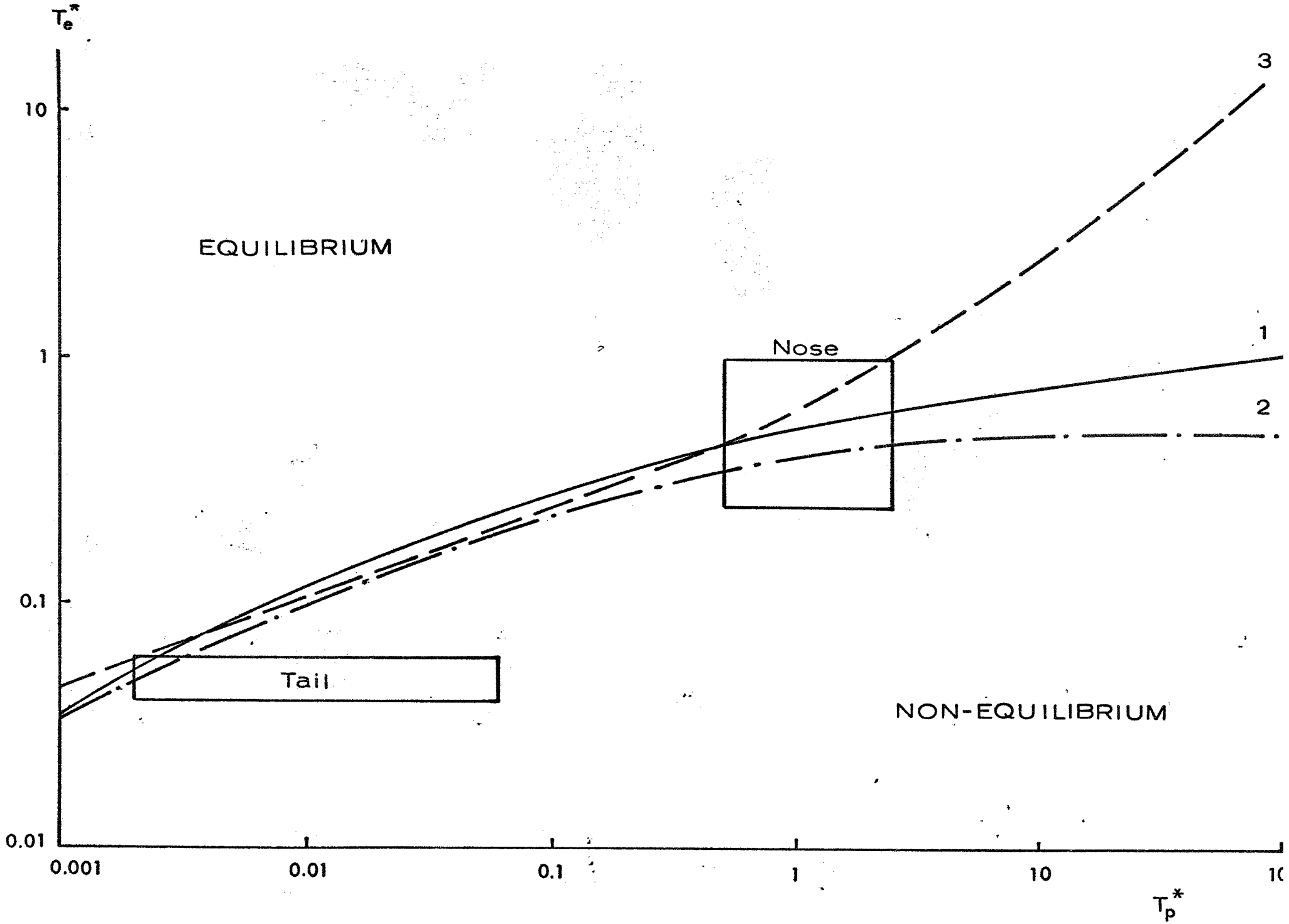
T_e^*
10
1
0.1
0.01
EQUILIBRIUM
Nose
Tail
NON-EQUILIBRIUM
3
1
2
0.001
0.01
0.1
1
10
T_p^*

FIGURE 3

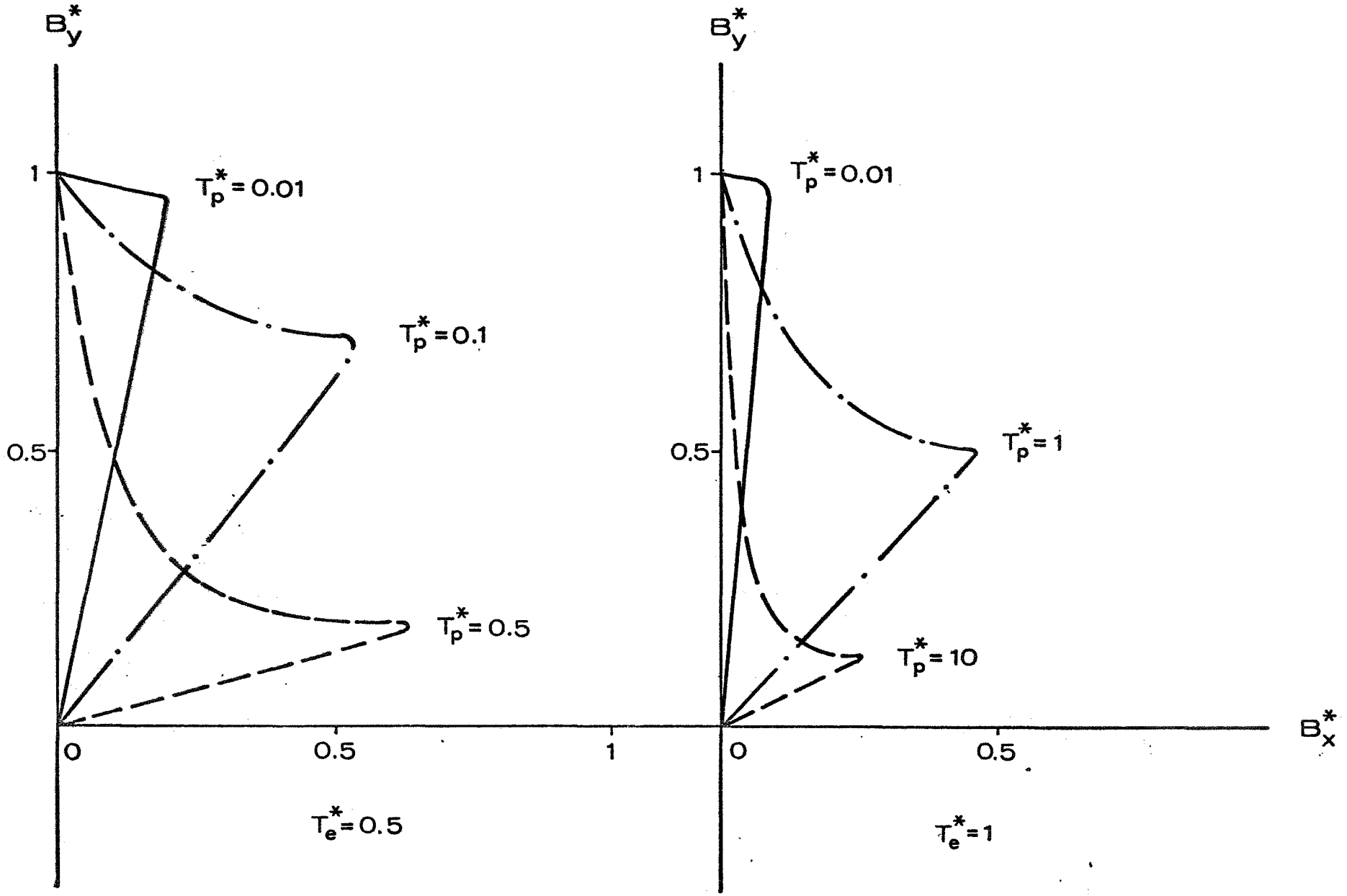
B_y^*
1
0.5
$T_p^* = 0.01$
$T_p^* = 0.1$
$T_p^* = 0.5$
0
0.5
1
$T_e^* = 0.5$
B_y^*
1
0.5
$T_p^* = 0.01$
$T_p^* = 1$
$T_p^* = 10$
0
0.5
B_x^*
$T_e^* = 1$

FIGURE 4